**Original papers**
***Manufacturing processes and systems***

УДК 544.16:544.723 DOI: 10.17277/jamt-2025-10-02-141-153

# Theoretical investigation of the interaction mechanism of trialkylamine derivatives with the copper phthalocyanine surface

**© Andrey A. Degtyarev[a]✉, Alexandra V. Trishina[a], Dariya P. Rostova[a]**

[a] *Tambov State Technical University, Bld. 2, 106/5, Sovetskaya St., Tambov, 392000, Russian Federation*

✉ ad.dycost@gmail.com

**Abstract:** The paper presents a theoretical study of the sorption mechanisms of tripropylamine, triisopropylamine, trihydroxypropylamines, and tetrapropylammonium chloride on the surface of copper phthalocyanine containing a metal atom, using density functional theory. The critical points of QTAIM, IRI, and charge distributions in sorbate-sorbent complexes were analyzed to investigate the interaction mechanism between the sorbate molecule and the surface. It was found that trialkylamines exhibit a higher binding energy with the surface than trialkylaminoalcohols due to their lower interaction energy with the solvent. In all cases, the binding of sorbate molecules to the surface is primarily driven by electrostatic and dispersion interactions; however, the presence of bonds with orbital overlap significantly enhances the stability of the complexes. The complex with the quaternary ammonium salt is the most stable due to a combination of electrostatic and orbital interactions. In the complex with a quaternary ammonium cation, significant polarization of the surface toward the crystal interior is observed, which may increase the interaction energy between molecules in the surface layers and reduce the solubility of modified particles in polar solvents. In all complexes with orbital overlap, the $3d_{z^2}$ -orbitals of the copper atom contribute from the surface side.

**Keywords:** copper phthalocyanine; DFT; adsorption; trialkylamines; QTAIM; IRI; surface modification.

**For citation:** Degtyarev AA, Trishina AV, Rostova DP. Theoretical investigation of the interaction mechanism of trialkylamine derivatives with the copper phthalocyanine surface. *Journal of Advanced Materials and Technologies*. 2025;10(2):141-153. DOI: 10.17277/jamt-2025-10-02-141-153

# Теоретическое изучение механизма взаимодействия производных триалкиламинов с поверхностью фталоцианина меди

**© А. А. Дегтярев[a]✉, А. В. Тришина[a], Д. П. Ростова[a]**

[a] *Тамбовский государственный технический университет, ул. Советская, 106/5, пом. 2, Тамбов, 392000, Российская Федерация*

✉ ad.dycost@gmail.com

**Аннотация:** Проведено теоретическое исследование механизмов сорбции трипропиламина, триизопропиламина, тригидроксипропиламинов и хлорида тетрапропиламмония на поверхности фталоцианина меди, включающей атом металла на уровне теории функционала плотности. В качестве инструментов изучения механизма взаимодействия молекулы сорбата с поверхностью использовались критические точки QTAIM, IRI и распределения зарядов в комплексах сорбат-сорбент. Определено, что триалкиламины имеют более высокую энергию связи с поверхностью, чем триалкиламиноспирты, за счет меньшей энергии взаимодействия с растворителем. Во всех случаях связь молекул сорбата с поверхностью в основном имеет электростатический и дисперсионный механизм, однако присутствие связей с перекрытием орбиталей существенно увеличивает стабильность комплексов. Комплекс с солью четвертичного аммониевого основания является самым стабильным за счет сочетания электростатического и орбитального механизмов. В комплексе с четвертичным аммониевым катионом наблюдается существенная поляризация поверхности по направлению вглубь кристалла, что может увеличивать энергию взаимодействия между молекулами в приповерхностных слоях и уменьшать растворимость модифицированных таким образом частиц в полярных растворителях. Во всех комплексах с перекрытием орбиталей со стороны поверхности участвует $3d_{z^2}$ -орбитали атома меди.

**Ключевые слова:** фталоцианин меди; DFT; адсорбция; триалкиламины; QTAIM; IRI; модификация поверхности.

**Для цитирования:** Degtyarev AA, Trishina AV, Rostova DP. Theoretical investigation of the interaction mechanism of trialkylamine derivatives with the copper phthalocyanine surface. *Journal of Advanced Materials and Technologies*. 2025;10(2):141-153. DOI: 10.17277/jamt-2025-10-02-141-153

## 1. Introduction

Surface modification of pigments is widely used to impart specific characteristics, including surface morphology, crystalline structure and particle size, optical properties, and the rheological characteristics of coatings and paints (CPs) formulated with these pigments [1].

Among the most commonly used surface modifiers are various surfactants (SAs) [2–5], high-molecular-weight substances [3–5], silicon oxide [3–4], as well as chemical functionalization of the surface, such as sulfo groups [6].

For pigments used in liquid CP formulations, the primary property determining pigment affinity for the binder is the oleophilic-hydrophilic balance of the surface. The higher the surface affinity, the easier the pigment disperses and the more stable the CPs formed with it are against sedimentation. When using acrylic, polyurethane, and other water-based coatings, efforts are made to increase surface hydrophilicity, whereas for alkyd coatings, oleophilicity is preferred.

Copper phthalocyanine (phthalocyanine blue pigment) is one of the most widely used organic pigments and is commonly used in CPs with alkyd binders. Although its surface is primarily oleophilic, it contains regions capable of adsorbing water molecules and other polar substances [7–8]. This can lead to difficulties in obtaining stable suspensions in alkyd binders when moisture impurities are present in the pigment itself or in auxiliary substances [9]. These regions can be shielded by adsorbing surfactants onto them. The most promising surfactants for this purpose include trialkylamines, quaternary ammonium bases, and their derivatives [10].

This study focuses on investigating the interaction mechanism of trialkylamines and some of their derivatives with the surface of copper phthalocyanine containing a metal atom, as this is the only part of the surface requiring shielding of hydrophilic sites [11]. Understanding the fundamental principles of the interaction mechanism between surfactants and the pigment surface will aid in selecting the optimal modifier for specific applications and producing materials with the desired properties.

The selected surfactants must perform well in both alkyd and aqueous environments (e.g., wet pigment or flash paste production). Surfactants are generally water-soluble, and their adsorption from an aqueous medium is of particular interest because if they adsorb well from water, they will also adsorb well from an alkyd medium and onto dry pigment. Therefore, this study will focus on the adsorption mechanism of surfactants from an aqueous medium onto the pigment surface. The structure of copper phthalocyanine was assumed to correspond to the β-modification, as this is the most commonly used form in pigment applications.

## 2. Materials and Methods

For this study, trialkylamines and their derivatives with a three-carbon chain length were selected, as tripropylamine is the first in the series of unbranched trialkylamines that adsorbs onto the copper phthalocyanine surface with a negative Gibbs free energy [11]. The structural formulas of the studied surfactants are as follows:

– Tripropylamine

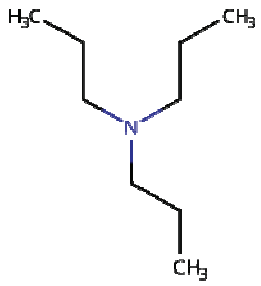


– Triisopropylamine

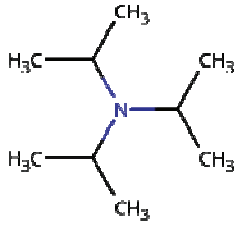


– Tris(1-hydroxypropyl)amine

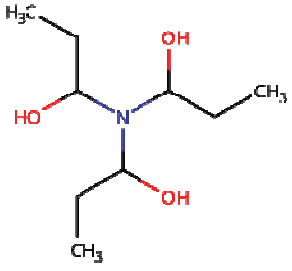

– Tris(2-hydroxypropyl)amine

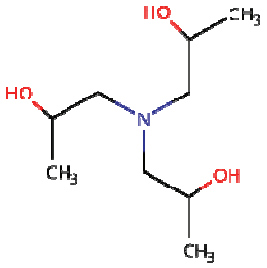

– Tetrapropylammoniumchloride

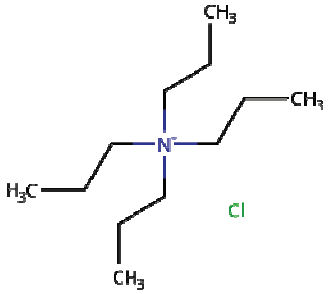

For hydroxypropylamines, two adsorption configurations were considered: with hydroxyl groups oriented toward and away from the surface.

For tetrapropylammonium chloride, hydrolysis of the molecule into a cation and chloride ion is possible:

$$\mathrm{TetPACl} \overset{K_1}{\Leftrightarrow} \mathrm{TetPA^+ + Cl^-}. \qquad (1)$$

Since tetrapropylammonium chloride is a salt of a strong acid and a weak base, the resulting cation recombines with a water molecule to form tetrapropylammonium hydroxide:

$$\mathrm{TetPA^+ + H_2O \Leftrightarrow TetPAOH + H^+}. \qquad (2)$$

The overall reaction (1), (2) can be expressed as:

$$\mathrm{TetPACl + H_2O \Leftrightarrow TetPAOH + H^+ + Cl^-}. \qquad (3)$$

At the same time, tetrapropylammonium hydroxide itself undergoes hydrolysis:

$$\mathrm{TetPAOH} \overset{K_2}{\Leftrightarrow} \mathrm{TetPA^+ + OH^-}. \qquad (4)$$

Thus, in aqueous solution, tetrapropylammonium can exist in three forms: chloride, hydroxide, and cationic. Their concentrations can be estimated using the dissociation constants of chloride and hydroxide ($K_1$ and $K_2$). While these values are not available for tetrapropylammonium, they are known for the structurally and chemically similar tetrabutylammonium: $K_1 = 0.24$; $K_2 = 0.011$ mol·L$^{-1}$ at 298 K [12].

The equilibrium constant for the overall reaction (3) is given by:

$$K = \frac{C_{\mathrm{TetAOH}} \times C_{\mathrm{H^+}} \times C_{\mathrm{Cl^-}}}{C_{\mathrm{TetACl}} \times C_{\mathrm{H_2O}}} = \frac{K_1}{K_2} \frac{10^{-14}}{C_{\mathrm{H_2O}}} =$$

$$= 3.93 \times 10^{-15} \text{ mol·L}^{-1} \text{ (298 K)}, \qquad (5)$$

indicating a very low final concentration of hydroxide.

Additionally, this can be demonstrated by assuming an initial tetrapropylammonium chloride concentration of up to 5 % by mass (which is typically the maximum surfactant concentration in industrial processes involving organic pigments), corresponding to a molar concentration of 0.225 mol·L$^{-1}$. Solving the equilibrium and mass balance equations simultaneously, the results are presented in Fig. 1.

Under these conditions, the concentration of tetrapropylammonium hydroxide does not exceed $4 \cdot 10^{-7}$ mol·L$^{-1}$. Therefore, only the adsorption of the chloride and cation species was considered in further analysis.

The copper phthalocyanine surface was modeled using a cluster consisting of four molecules. The cluster geometry was based on experimental data for the β-crystal modification [13], with all non-hydrogen atoms fixed during geometry optimization to maintain consistency with the crystal lattice structure. The optimization process involved adjusting the position of the sorbate molecule relative to the surface, along with its internal coordinates.

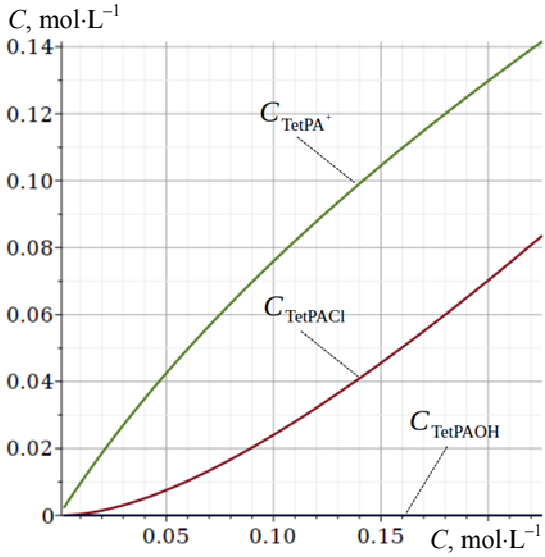


**Fig. 1.** Concentrations of tetrapropylammonium in the forms of chloride, hydroxide, and cation at an initial tetrapropylammonium chloride concentration of up to 0.225 mol·L$^{-1}$

To model the adsorption process, a two-layer ONIOM scheme [14] was employed. The surfactant molecules and the two nearest copper phthalocyanine molecules were treated with a high-level method, while the remaining two molecules were modeled using a low-level method. The extended tight-binding (XTB2) method [15] was used for the low-level calculations, while density functional theory (DFT) was employed for the high-level calculations. Specifically, the r$^2$SCAN-3c composite method [16] was used for geometry optimization, and single-point energy calculations were performed using the ωB97x/def2-SVPD method [17–19].

The solvent was modeled using the continuum ALPB approach [20]. All geometry optimizations and wavefunction calculations were conducted using the ORCA 6 software package [21].

To determine the interaction mechanisms within the sorbate-sorbent complexes, the following approaches were used:

– Bader's Atoms in Molecules (QTAIM) theory [22, 23];

– Interaction Region Indicator (IRI) [24];

– Charge distribution analysis using the Hirshfeld [25], Bader (AIM) [22], and CHELPG [26] methods.

All calculations related to the interaction mechanism were performed using the Multiwfn software package [27], based on molecular orbitals obtained from single-point calculations.

QTAIM analysis allows for the identification of critical points corresponding to the maximum electron density at the boundary between two atomic basins, known as bond critical points (BCPs, type (3, –1)). The presence of these points confirms the existence of a bond between two atoms. The nature and characteristics of this bond can be assessed by evaluating key parameters at the BCP, including:

– Electron density ($\rho_{BCP}$);

– Electron localization function ($ELF_{BCP}$) [28];

– Localized orbital locator ($LOL_{BCP}$) [29];

– The product of the second Hessian eigenvalue sign and electron density ($sign(\lambda_2)\times\rho_{BCP}$) [24];

– Lagrangian kinetic energy density ($G_{BCP}$) and potential energy density ($V_{BCP}$).

For hydrogen bonds, the bond energy (kJ·mol$^{-1}$) can be estimated from the electron density using the equation [30]:

$$E_H \approx -933.33\,\rho_{BCP} + 3.11. \quad (6)$$

$ELF_{BCP}$ and $LOL_{BCP}$ values close to 1 (0.8–1.0) indicate covalent bonding, while values below 0.5 suggest non-covalent interactions.

A negative $sign(\lambda_2)\times\rho_{BCP}$ value confirms a bonding interaction, with its magnitude reflecting bond strength. A $\rho_{BCP} \approx 0$ value near zero is characteristic of van der Waals interactions [24]. Hydrogen bonds exhibit $\rho_{BCP}$ values of approximately 0.02–0.05 for classical, 0.05–0.09 for strong, and 0.09–0.12 for very strong interactions [31]. Halogen, pnictogen, and other donor-acceptor non-covalent bonds have a broader $\rho_{BCP}$ range (0.004–0.12), but within a specific bond type, $\rho_{BCP}$ and bond energy are typically linearly correlated [32, 33].

Reference [32] categorizes non-covalent interactions based on the $(|V|/G)_{BCP}$ ratio:

– $(|V|/G)_{BCP} < 1$ as $\rho_{BCP}$ increases, interactions resemble ionic (closed-shell) bonds;

– $1 < (|V|/G)_{BCP} < 2$ – intermediate bonds;

– $2 < (|V|/G)_{BCP}$ – as $\rho_{BCP}$ increases, interactions resemble covalent (shared-shell) bonds.

A comprehensive analysis of donor-acceptor interactions in [33] provides correlation equations for bond energy as a function of $\rho_{BCP}$ for three bond types:

– Closed-shell

$$E_B \approx -2768\,\rho_{BCP} + 2.1; \quad (7)$$

– Intermediate

$$E_B \approx -1487\,\rho_{BCP} + 6.5; \quad (8)$$

– Shared-shell

$$E_B \approx -857\,\rho_{BCP} - 0.4. \quad (9)$$

As seen from equations (7) – (9), hydrogen bonds, which are described by equation (6), are closer to shared-shell interactions, meaning they tend to form molecular orbitals in the space between bonded nuclei.

Only the critical points connecting the sorbate molecule to the copper phthalocyanine cluster were analyzed.

The contributions of individual orbitals to bond formation were also assessed using a localized molecular orbital (LMO) decomposition at the critical point. The Pipek-Mezey localization method with Mulliken population analysis was used in this study [34, 35].

The IRI index highlights regions of attractive or repulsive interactions. In these regions, the IRI parameter, calculated using equation (10), approaches

zero, while the $\text{sign}(\lambda_2)\times\rho(r)$ value indicates interaction strength and direction.

$$\text{IRI}(r) = \frac{|\nabla\rho(r)|}{\rho(r)^{1.1}}. \quad (10)$$

Charge distribution analysis helps evaluate electrostatic interactions between the surface and the sorbed molecule. Charges were computed for the high-level region from the wavefunction obtained using the ωB97x/def2-SVPD method. The atomic charges were determined for the surface copper atom interacting with the sorbate, nitrogen and chlorine atoms (for tetrapropylammonium chloride), and the molecular fragments forming the sorbate-sorbent complex:

– Frag. 1 – subsurface copper phthalocyanine molecule;

– Frag. 2 – copper phthalocyanine molecule in direct contact with the sorbate;

– Frag. 3 – sorbate molecule.

Additionally, for all sorbate-sorbent complexes, formation energy was evaluated at the r$^2$SCAN-3c theoretical level.

Visualizations were created using the VMD software [36].

## 3. Results and Discussion

The description of the obtained complexes and their formation energies are presented in Table 1, and their structures are shown in Fig. 2.

Tetrapropylammonium chloride has the highest binding energy to the surface. The tetrapropylammonium cation and both isomers of tripropylamine have approximately three times lower binding energy. Amino alcohols exhibit the weakest interaction with the surface among the studied surfactants, which can be explained by the hydrophilic OH groups increasing their interaction energy with the solvent. This, in turn, makes adsorption onto the pigment surface less favorable.

For the (3, –1) critical points, the values of electron density, $\text{ELF}_{\text{BCP}}$ and $\text{LOL}_{\text{BCP}}$, $G_{\text{BCP}}$ and $V_{\text{BCP}}$ energy densities were calculated, along with the estimated bond energies assuming hydrogen bonding (2) and using generalized formulas for weak interactions (3) – (5). All values a represented in Table 2.

The $(|V|/G)_{\text{BCP}}$ values indicate that nearly all intermolecular interactions in the studied complexes are predominantly electrostatic in nature. This conclusion is further supported by the low ELF and LOL values at the critical points. Only four bonds, found in complexes 1, 2, 5, and 7, exhibit $(|V|/G)_{\text{BCP}} \geq 1$, all of which involve the interaction between a surface copper atom and an atom within the surfactant molecule. Comparing the complex numbers with their formation energies from Table 1 reveals that the complexes containing a BCP with $(|V|/G)_{\text{BCP}} \geq 1$ have higher binding energies than those without such interactions (except for the complex with the cation).

**Table 1.** The formation energy of sorbate-sorbent complexes of the studied surfactants with a copper phthalocyanine cluster

| Complex No. | Sorbate type and its location | Sorption energy | Cu-N distance between the sorbate and the surface, Å |
|---|---|---|---|
| 1 | tripropylamine | –48.03 | 3.235 |
| 2 | triisopropylamine | –48.52 | 4.252 |
| 3 | tris-(1-hydroxypropyl)amine, OH towards the surface | –30.08 | 4.772 |
| 4 | tris-(1-hydroxypropyl)amine, OH away from the surface | –33.20 | 3.729 |
| 5 | tris-(2-hydroxypropyl)amine, OH towards the surface | –46.18 | 4.131 |
| 6 | tris-(2-hydroxypropyl)amine, OH away from the surface | –39.00 | 3.719 |
| 7 | tetrapropylammonium chloride | –158.09 | 5.946 |
| 8 | tetrapropylammonium cation | –50.59 | 5.707 |

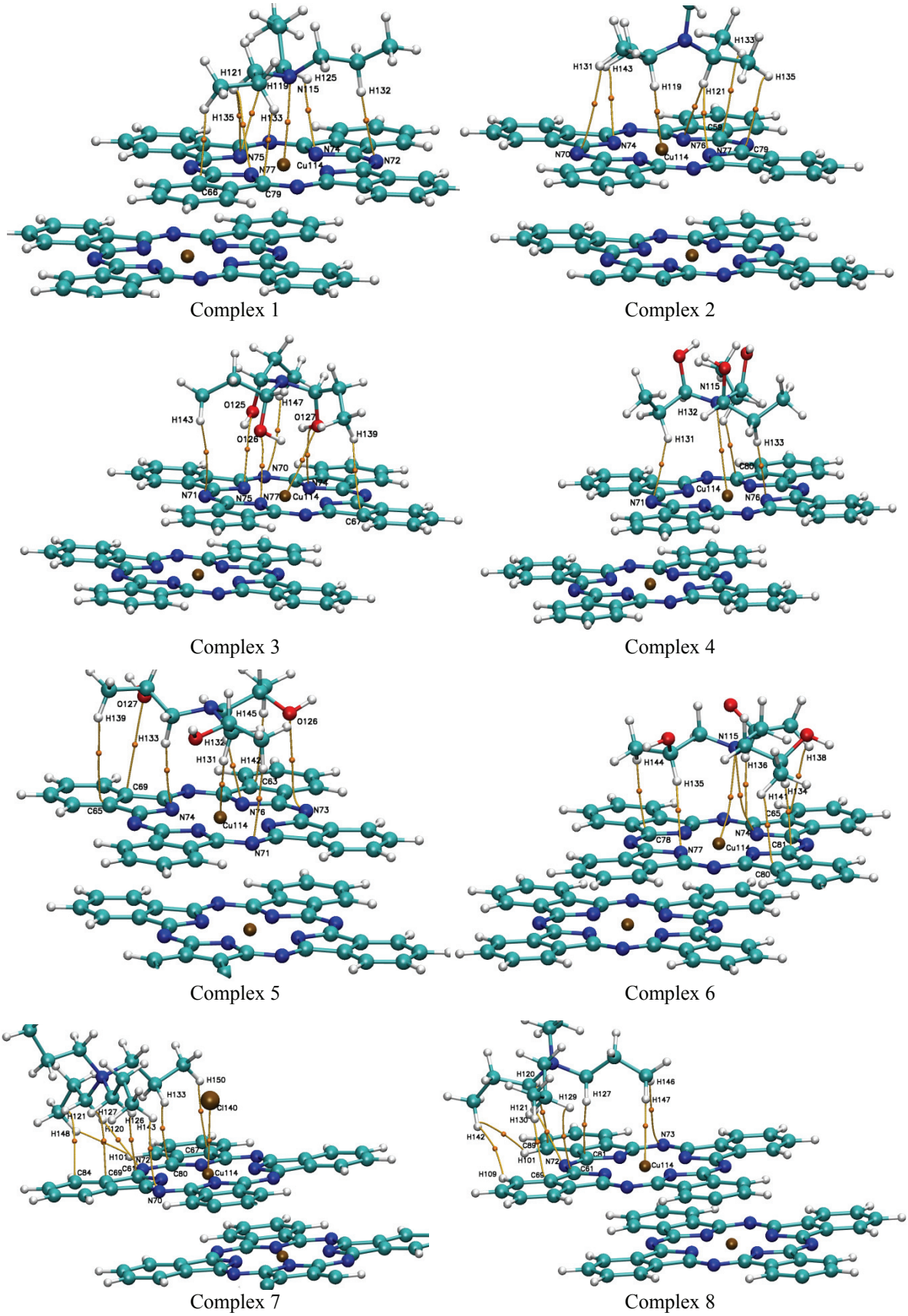


**Fig. 2.** The structure of sorbate-sorbent complexes of the studied surfactants with a copper phthalocyanine cluster is shown, with critical points (3, –1) for intermolecular interactions between the sorbate and the surface, and pathways connecting them to the points (3, –3)

**Table 2.** Characteristics of BCP binding the sorbent molecule and the surface

| Complex No. | Interacting atoms | The distance between atoms, Å | $\rho_{BCP}$ | $(\lvert V\rvert/G)_{BCP}$ | $ELF_{BCP}$ | $LOL_{BCP}$ | $E_H$ | $E_B$ |
|---|---|---|---|---|---|---|---|---|
| 1 | 2 | 3 | 4 | 5 | 6 | 7 | 8 | 9 |
| 1 | C66-H135 | 2.701 | 0.00757 | 0.81 | 0.0268 | 0.1426 | –3.95 | –18.84 |
| | N77-H121 | 3.178 | 0.00342 | 0.71 | 0.0080 | 0.0829 | –0.09 | –7.38 |
| | C79-H133 | 2.705 | 0.00678 | 0.75 | 0.0187 | 0.1216 | –3.22 | –16.66 |
| | N75-H121 | 3.229 | 0.00292 | 0.67 | 0.0068 | 0.0766 | 0.39 | –5.98 |
| | N75-H119 | 2.718 | 0.00756 | 0.86 | 0.0251 | 0.1384 | –3.95 | –18.84 |
| | Cu114-N115 | 3.235 | 0.00806 | 1.00 | 0.0293 | 0.1483 | –4.41 | –5.41 |
| | N74-H125 | 2.730 | 0.00768 | 0.85 | 0.0250 | 0.1381 | –4.05 | –19.15 |
| | N72-H132 | 2.690 | 0.00719 | 0.90 | 0.0240 | 0.1357 | –3.60 | –17.81 |
| 2 | C79-H135 | 3.014 | 0.00471 | 0.69 | 0.0138 | 0.1062 | –1.29 | –10.94 |
| | N77-H121 | 2.814 | 0.00638 | 0.81 | 0.0191 | 0.1227 | –2.85 | –15.56 |
| | Cu114-H119 | 2.527 | 0.01125 | 1.10 | 0.0407 | 0.1710 | –7.39 | –10.13 |
| | N76-H121 | 2.746 | 0.00703 | 0.84 | 0.0225 | 0.1321 | –3.45 | –17.35 |
| | C59-H133 | 3.287 | 0.00258 | 0.66 | 0.0064 | 0.0749 | 0.71 | –5.03 |
| | N70-H131 | 3.439 | 0.00173 | 0.63 | 0.0034 | 0.0555 | 1.50 | –2.68 |
| | N74-H143 | 2.875 | 0.00614 | 0.82 | 0.0185 | 0.1210 | –2.62 | –14.89 |
| | N71-H143 | 3.452 | 0.00159 | 0.60 | 0.0031 | 0.0535 | 1.63 | –2.30 |
| 3 | N77-O126 | 3.006 | 0.00837 | 0.84 | 0.0193 | 0.1233 | –4.70 | –21.06 |
| | N75-O125 | 3.143 | 0.00685 | 0.82 | 0.0149 | 0.1097 | –3.28 | –16.86 |
| | Cu114-O127 | 3.162 | 0.00724 | 0.90 | 0.0176 | 0.1181 | –3.64 | –17.93 |
| | N74-O127 | 3.200 | 0.00682 | 0.79 | 0.0152 | 0.1108 | –3.26 | –16.78 |
| | C67-H139 | 3.143 | 0.00354 | 0.74 | 0.0086 | 0.0857 | –0.20 | –7.71 |
| | N70-H147 | 3.355 | 0.00189 | 0.64 | 0.0039 | 0.0595 | 1.35 | –3.12 |
| 4 | N71-H131 | 2.615 | 0.00871 | 0.90 | 0.02892 | 0.14738 | –5.02 | –22.02 |
| | Cu114-N115 | 3.729 | 0.00330 | 0.70 | 0.01062 | 0.09429 | 0.03 | –7.02 |
| | N76-H133 | 2.513 | 0.01060 | 0.94 | 0.04046 | 0.17055 | –6.78 | –27.24 |
| | C80-H132 | 2.630 | 0.00835 | 0.79 | 0.02321 | 0.13375 | –4.68 | –21.00 |
| | N71-H142 | 2.865 | 0.00486 | 0.82 | 0.01419 | 0.10742 | –1.43 | –11.37 |
| 5 | Cu114-H131 | 2.615 | 0.00965 | 1.00 | 0.03282 | 0.15574 | –5.89 | –7.76 |
| | N73-O126 | 3.730 | 0.00238 | 0.66 | 0.00504 | 0.06684 | 0.89 | –4.49 |
| | N76-H132 | 2.567 | 0.00947 | 0.91 | 0.03561 | 0.16141 | –5.73 | –24.12 |
| | N74-H133 | 2.730 | 0.00718 | 0.88 | 0.02505 | 0.13839 | –3.59 | –17.77 |
| | C63-H145 | 2.929 | 0.00483 | 0.77 | 0.01591 | 0.11312 | –1.40 | –11.28 |
| | C65-H139 | 3.688 | 0.00120 | 0.56 | 0.00285 | 0.05141 | 1.99 | –1.23 |
| | C69-O127 | 3.858 | 0.00189 | 0.64 | 0.00437 | 0.06260 | 1.34 | –3.14 |
| | C78-H144 | 2.884 | 0.00532 | 0.72 | 0.01646 | 0.11483 | –1.86 | –12.63 |
| | N77-H135 | 2.769 | 0.00652 | 0.85 | 0.02155 | 0.12947 | –2.97 | –15.94 |
| 6 | Cu114-N115 | 3.719 | 0.00360 | 0.69 | 0.01272 | 0.10237 | –0.25 | –7.87 |
| | N74-N115 | 3.723 | 0.00356 | 0.68 | 0.01300 | 0.10341 | –0.21 | –7.75 |
| | C80-H136 | 2.584 | 0.00886 | 0.83 | 0.03023 | 0.15026 | –5.16 | –22.43 |
| | C67-H141 | 2.935 | 0.00545 | 0.76 | 0.01752 | 0.11809 | –1.97 | –12.98 |
| | C81-H134 | 2.654 | 0.00772 | 0.80 | 0.02334 | 0.13410 | –4.09 | –19.27 |
| | C65-H138 | 2.989 | 0.00505 | 0.74 | 0.01620 | 0.11402 | –1.61 | –11.89 |
| 7 | Cl140-Cu114 | 3.133 | 0.01350 | 1.19 | 0.05466 | 0.19402 | –9.49 | –13.46 |
| | H143-N70 | 3.025 | 0.00420 | 0.74 | 0.01152 | 0.09773 | –0.81 | –9.52 |
| | H150-C67 | 3.133 | 0.00334 | 0.72 | 0.00986 | 0.09111 | 0.00 | –7.13 |

*Continuation Table 2*

| 1 | 2 | 3 | 4 | 5 | 6 | 7 | 8 | 9 |
|---|---|---|---|---|---|---|---|---|
| 7 | H133-C81 | 2.813 | 0.00624 | 0.71 | 0.01767 | 0.11849 | –2.72 | –15.18 |
| | H126-C61 | 2.766 | 0.00614 | 0.76 | 0.01781 | 0.11891 | –2.62 | –14.91 |
| | N72-H120 | 2.629 | 0.00772 | 0.89 | 0.02805 | 0.14545 | –4.10 | –19.28 |
| | H127-C69 | 3.040 | 0.00499 | 0.72 | 0.01698 | 0.11649 | –1.55 | –11.72 |
| | H148-H101 | 2.579 | 0.00278 | 0.62 | 0.00635 | 0.07440 | 0.52 | –5.59 |
| 8 | H121-C84 | 2.996 | 0.00492 | 0.69 | 0.01777 | 0.11889 | –1.49 | –11.53 |
| | N73-H146 | 3.160 | 0.00322 | 0.74 | 0.00752 | 0.08039 | 0.10 | –6.82 |
| | Cu114-H147 | 2.746 | 0.00731 | 0.91 | 0.02333 | 0.13410 | –3.71 | –18.13 |
| | C81-H127 | 2.692 | 0.00745 | 0.79 | 0.02173 | 0.12991 | –3.85 | –18.53 |
| | C61-H129 | 2.912 | 0.00542 | 0.71 | 0.01657 | 0.11516 | –1.95 | –12.91 |
| | N72-H121 | 2.612 | 0.00823 | 0.90 | 0.03131 | 0.15263 | –4.58 | –20.69 |
| | C69-C130 | 2.886 | 0.00634 | 0.76 | 0.02167 | 0.12981 | –2.81 | –15.45 |
| | C89-H120 | 3.015 | 0.00463 | 0.72 | 0.01685 | 0.11611 | –1.21 | –10.72 |
| | H101-H142 | 2.640 | 0.00338 | 0.63 | 0.00946 | 0.08939 | –0.04 | –7.25 |
| | H109-H142 | 3.328 | 0.00060 | 0.43 | 0.00119 | 0.03427 | 2.55 | 0.45 |

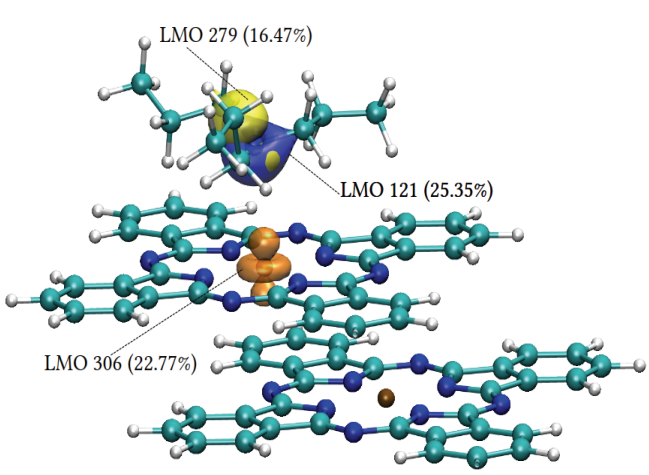


Complex 1 (Cu114-N115)

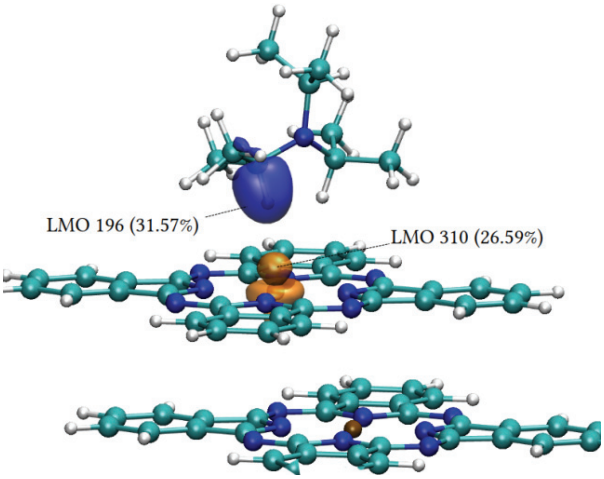


Complex 2 (Cu114-H119)

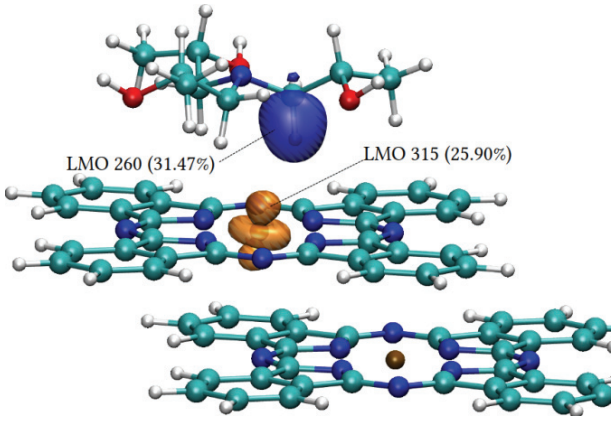


Complex 5 (Cu114-H131)

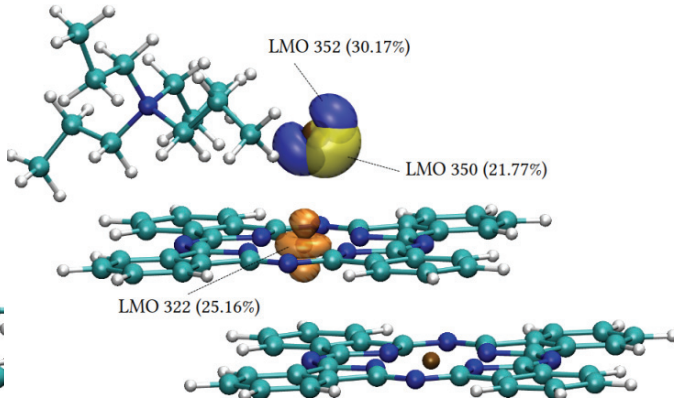


Complex 7 (Cu114-Cl140)

**Fig. 3.** LMO involved in interactions with $(|V|/G)_{BCP} \geq 1$, isosurface at 0.1 a.u.

Letus take a closer look at the interactions where $(|V|/G)_{BCP} \geq 1$. Since these interactions are of an intermediate type, possessing both orbital and electrostatic contributions, it is useful to examine the orbitals involved in their formation. Figure 3 presents the contributions of localized molecular orbitals (LMOs) to the BCP of these interactions, displaying orbitals with contributions exceeding 10 %.

As shown in Figure 3, in all of the presented interactions, the copper atom's $3d_{z^2}$ -orbital is involved from the surface side, which can be recognized by its characteristic shape. The contribution from this orbital remains constant at around 25 %.

On the sorbate side, in two cases, the molecular orbitals of the C–H bond are involved in the interaction (complexes 2 and 5). In complex 5, a reorientation of the copper $3d_{z^2}$ -orbital (LMO 315) occurs toward the sorbate molecular orbital (LMO 260). It is also worth noting that the interaction involves the C–H bond of the methylene group adjacent to the nitrogen atom, which is the most polarized.

In complexes 1 and 7, two orbitals are involved from the sorbate side. In complex 1, these are the lone electron pair of the nitrogen atom (LMO 121, 25.35 %) and the molecular orbital of the N–C bond (LMO 279, 16.47 %). In complex 7, these are the p-orbital (LMO 352, 30.17 %) and the sp-orbital (LMO 350, 21.77 %) of the chlorine atom (atomic orbital decomposition coefficients > 0.4 for the 3*s* and $3p_y$ electrons).

In complexes 4 and 6, the interaction involving the nitrogen lone pair is also present, but it is much weaker than in complex 1 and is based solely on the electrostatic mechanism. This is likely due to the distance factor; at $r = 3.2$ Å (complex 1), overlap with the copper $3d_{z^2}$ -orbitals is still possible, while at $r = 3.7$ Å (complexes 4 and 6), it is no longer possible. The critical distance for the overlap of copper $3d_{z^2}$ -orbitals and C–H molecular orbitals is around 2.6 Å (for complex 8, $r = 2.746$ Å and $(|V|/G)_{BCP} = 0.91$).

Thus, the presence of orbital interactions positively affects the stability of the sorbate-sorbent complexes, but it does not explain the high adsorption energy of tetra-n-propylammonium chloride, which is characteristic of chemisorption. However, the highest value of $\rho_{BCP} = 0.0135$ indicates a weak non-covalent interaction, which is further supported by the $ELF_{BCP}$ and $LOL_{BCP}$ values.

The sums of the $E_H$ and $E_B$ values for a single complex do not match the calculated adsorption energy. $\Sigma E_H$ always gives a lower value, while $\Sigma E_B$ gives an overestimated value, except for complex 7. The lower value of $\Sigma E_H$ can be explained by the fact that most interactions are far from those with a shared shell. The overestimated value of $\Sigma E_B$ can be explained by the influence of the solvent, as equations (3) – (5) were derived for the gas phase.

The results of the IRI calculations for the investigated complexes are shown in Fig. 4.

For complexes 1–2 and 7–8, all peak values in the binding region are within $\rho \approx 0$ to 0.01 a.u., as shown in Table 2. For complexes with amino alcohols (3–6), additional peaks are observed in the regions $\rho \approx 0.02$ a.u. (complexes with hydroxyl groups oriented toward the pigment surface) and $\rho \approx 0.017$ a.u. (complexes with hydroxyl groups oriented away from the pigment surface). To understand what these interactions are, let us construct a 3D map of the IRI parameter for one of these complexes (Fig. 5).

As seen in Figure 5, these peaks correspond to intramolecular H···OH bonds, so the corresponding critical points (3, –1) did not appear in the table for intermolecular interactions.

The presence of sufficiently extensive binding regions with $\rho \approx 0$ to 0.01 near nonpolar groups (Fig. 5) indicates the significant role of dispersion forces in the formation of sorbate-sorbent complexes.

The charges for the fragments, as well as the copper atom on the surface, and the nitrogen and chlorine atoms of the sorbate, are presented in Table 3.

For all the complexes of tertiary amines and amino alcohols, a similar pattern is observed. There is a slight polarization of the surface (using the Hirshfeld and AIM methods), with the subsurface molecule becoming positively charged and the surface negatively charged. Meanwhile, the sorbate molecule acquires a small negative charge (Hirshfeld and CHELPG methods) or remains neutral (AIM). When looking at the fragment charges, only the CHELPG method shows a small electrostatic interaction between the sorbate and the surface. Considering the centers of positive and negative charges – the copper atom on the surface and the nitrogen atom of the sorbate – attraction is possible in all cases (AIM shows almost quantitative charges of $Cu^+$ and $N^-$), but the distance between these centers is quite large (see Table 1), which hinders effective interaction.

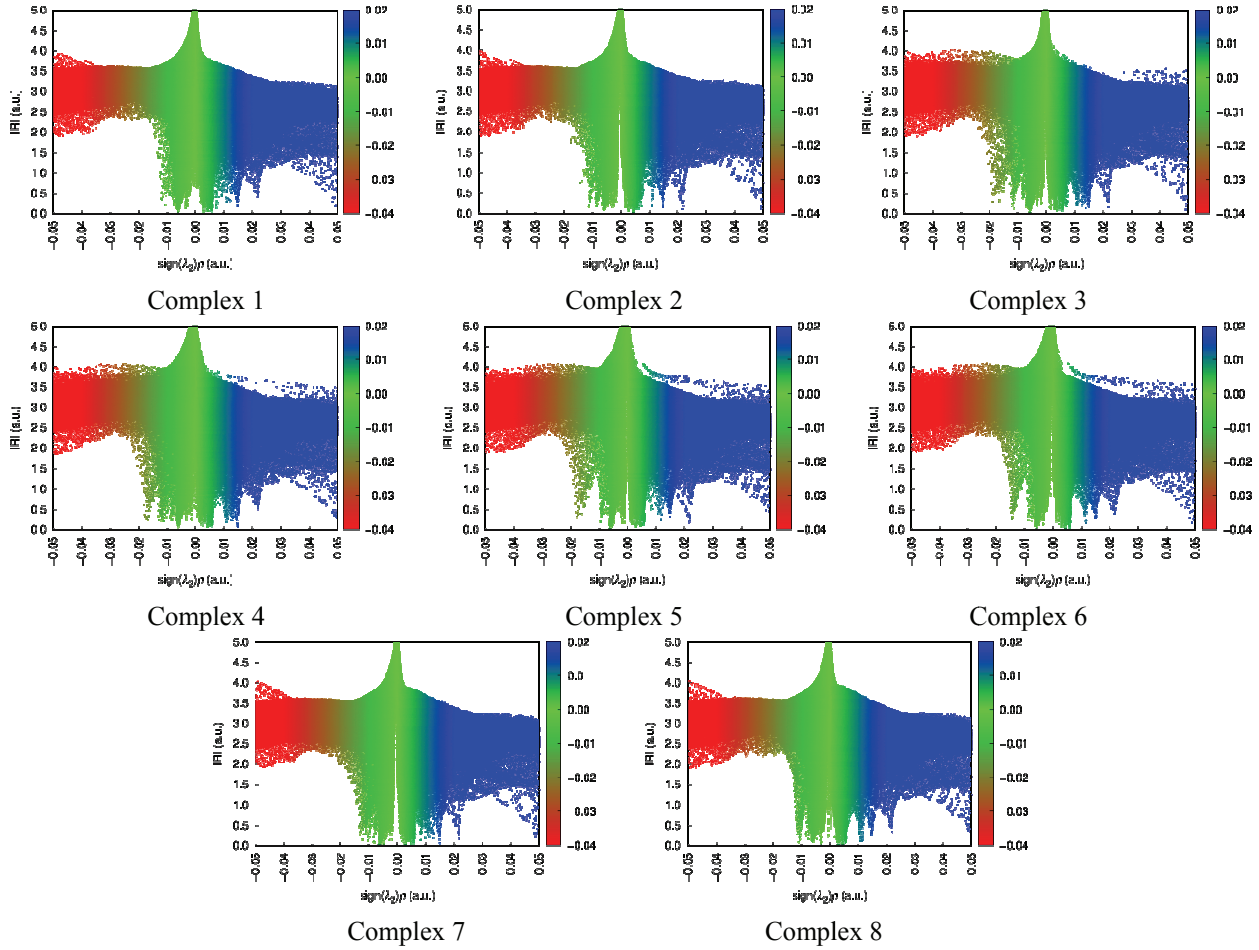


**Fig. 4.** IRI for sorbate-sorbent complexes

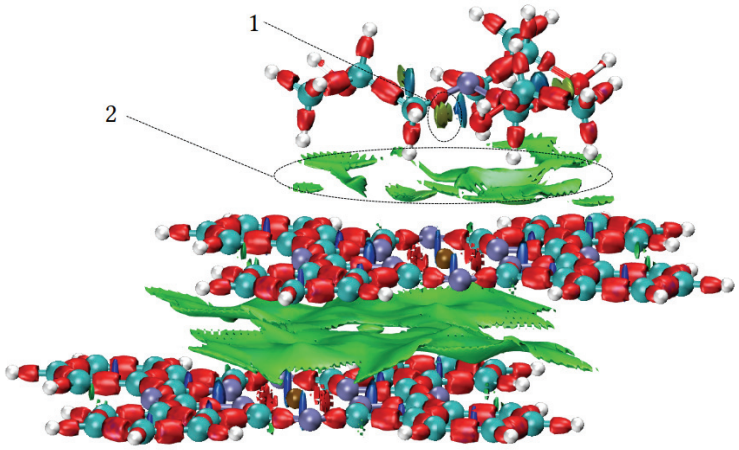


**Fig. 5.** Isosurface IRI = 1 for complex 5; *1* is the region of intramolecular hydrogen bonds in the sorbate molecule, *2* is the region of weak intermolecular interactions

For the tetra-n-propylammonium chloride complex, surface polarization is observed only when using the CHELPG method. It is noted that the occupancy of nitrogen and copper atoms is reduced compared to the average value for complexes 1–6, which, together with the shorter Cu–Cl distance compared to Cu–N, makes the electrostatic interaction between the chlorine atom and the surface more significant than that between the nitrogen atom and the surface in previous complexes.

For the tetra-n-propylammonium cation complex, the strongest surface polarization is observed. Both the Hirshfeld and CHELPG methods show charge transfer from the cation to the pigment

**Table 3.** Charge distribution in sorbate-sorbent complexes

| Complex No. | Hirshfeld method | | | | | | CHELPG method | | | | | | AIM method | | | | | |
|---|---|---|---|---|---|---|---|---|---|---|---|---|---|---|---|---|---|---|
| | Frag 1 | Frag 2 | Frag 3 | Cu114 | N115 | Cl | Frag 1 | Frag 2 | Frag 3 | Cu114 | N115 | Cl | Frag 1 | Frag 2 | Frag 3 | Cu114 | N115 | Cl |
| 1 | 0.17 | –0.10 | –0.07 | 0.36 | –0.09 | – | 0.09 | 0.13 | –0.22 | 0.66 | –0.65 | – | 0.18 | –0.19 | 0.01 | 1.04 | –1.14 | – |
| 2 | 0.21 | –0.12 | –0.09 | 0.34 | –0.10 | – | 0.13 | 0.09 | –0.22 | 0.71 | –0.98 | – | 0.22 | –0.22 | 0.00 | 0.99 | –1.16 | – |
| 3 | 0.21 | –0.17 | –0.03 | 0.35 | –0.11 | – | 0.12 | 0.06 | –0.19 | 0.65 | –0.76 | – | 0.22 | –0.21 | –0.01 | 1.01 | –1.18 | – |
| 4 | 0.25 | –0.15 | –0.10 | 0.34 | –0.10 | – | 0.17 | 0.07 | –0.24 | 0.67 | –0.98 | – | 0.26 | –0.26 | 0.00 | 1.00 | –1.18 | – |
| 5 | 0.13 | –0.08 | –0.06 | 0.35 | –0.11 | – | 0.06 | 0.11 | –0.17 | 0.68 | –0.73 | – | 0.14 | –0.15 | 0.01 | 1.01 | –1.12 | – |
| 6 | 0.19 | –0.08 | –0.11 | 0.35 | –0.10 | – | 0.11 | 0.12 | –0.23 | 0.70 | –0.86 | – | 0.19 | –0.19 | 0.00 | 1.02 | –1.12 | – |
| 7 | 0.00 | –0.01 | 0.01 | 0.38 | 0.10 | –0.66 | –0.08 | 0.20 | –0.13 | 0.71 | –0.27 | –0.82 | 0.00 | –0.04 | 0.03 | 1.10 | –1.09 | –0.89 |
| 8 | 0.59 | –0.40 | 0.81 | 0.26 | 0.10 | – | 0.55 | –0.21 | 0.65 | 0.59 | –0.06 | – | 0.61 | –0.57 | 0.96 | 0.89 | –1.10 | – |

surface. Based on the charges on fragments 2 and 3, substantial interaction is expected, and from the absence of orbital overlap bonds in this complex, it can be concluded that this interaction contributes significantly to the adsorption energy. Significant polarization directed into the surface may also increase the stability of copper phthalocyanine crystals through electrostatic interactions between the molecules. This effect can occur during the adsorption of any cations, but only cations whose interaction energy with the solvent is small enough to make adsorption favorable will effectively adsorb. This effect can be used to stabilize (reduce the solubility of) crystals in polar solvents.

## 4. Conclusion

Tertiary alkylamines generally have higher binding energy with the copper phthalocyanine surface in the aqueous phase than tertiary alkylamino alcohols due to their lower interaction energy with the solvent. The binding of sorbate molecules to the surface mainly involves electrostatic and dispersion mechanisms. However, the presence of bonds with orbital overlap significantly increases the stability of the complexes. Therefore, it can be concluded that for effective surfactant adsorption on the copper phthalocyanine surface, it is necessary to ensure the overlap of sorbate molecule orbitals with the $3d_{z^2}$-orbitals of the copper atom on the surface. The complex with a quaternary ammonium salt is the most stable due to the combination of electrostatic and orbital interaction mechanisms. In the complex with the charged particle – the quaternary ammonium cation – there is significant surface polarization directed deep into the crystal, which may increase the interaction energy between pigment molecules in the subsurface layers and reduce the solubility of the modified particles in polar solvents.

## 5. Funding

The study was funded by the Ministry of Education and Science of the Tambov Region, grant number MU2023-02/16 from the regional competition “Grants to Support Applied Scientific Research by Young Scientists in 2023”.

## 6. Conflict of interest

The authors declare no conflict of interest.

## References

1. Sarkodie B, Acheampong C, Asinyo B, Zhang X, et al. Characteristics of pigments, modification, and their functionalities. *Color Research & Application*. 2019;44(3):396-410. DOI:10.1002/col.22359

2. Sun S, Ding H, Zha Y, Chen W, et al. Surface organic modification of $CaCo_3$-$TiO_2$ composite pigment. *Minerals*. 2019;9(2):112. DOI:10.3390/min9020112

3. Švara Fabjan E, Otoničar M, Gaberšček M, Sever Škapin A. Surface protection of an organic pigment based on a modification using a mixed-micelle system. *Dyes and Pigments*. 2016;127:100-109. DOI:10.1016/j.dyepig.2015.12.016

4. Jadhav SA, Bongiovanni R, Marchisio DL, Fontana D, et al. Surface modification of iron oxide

($Fe_2O_3$) pigment particles with amino-functional polysiloxane for improved dispersion stability and hydrophobicity. *Pigment & Resin Technology*. 2014;43(4):219-227. DOI:10.1108/PRT-07-2013-0057

5. Karlsson P, Palmqvist AEC, Holmberg K. Surface modification for aluminium pigment inhibition. *Advances in Colloid and Interface Science*. 2006;128-130:121-134. DOI:10.1016/j.cis.2006.11.010

6. Rostami M, Khosravi A, Attar MM. Synthesis and surface modification of Pigment Red 3 by sulfonation method for improving properties in waterborne ink. *Progress in Color, Colorants and Coatings*. 2017;10(1): 51-65. DOI:10.30509/pccc.2017.75714

7. Degtyarev AA, Trishina AV, Tarakanov AG. Research of the sorption activity of copper phthalocyanine. *Butlerovskie Soobshcheniya = Butlerov Communications*. 2018;55(7):22-30.(In Russ.)

8. Degtyarev AA, Zarapina IV, Zdereva AV. Modeling the sorption of low-molecular compounds on the surface of copper phthalocyanine by the method of density functional theory. *Butlerovskie Soobshcheniya = Butlerov Communications*. 2021;65(3):86-92. (In Russ.) DOI: 10.37952/ROI-jbc-01/21-65-3-86

9. Lambourne R, Strivens TA. *Paint and surface coatings: theory and practice*. Elsevier Science; 1999. 784 p.

10. Degtyarev AA, Trishina AV, Dyachkova TP, Subocheva MYu, et al. Predicting the possibility of oleophilizing surfaces of copper phthalocianin on the basis of reactivity descriptors. *Russian Journal of Physical Chemistry A*. 2020;94(8):1694-1698. DOI:10.1134/ S0036024420080051

11. Degtyarev AA, Trishina AV, Kroviakova EI. Study of the trialkylamines adsorption on the surface of copper phthalocyanine using density functional theory methods. *Journal of Advanced Materials and Technologies*. 2024;9(4):286-295. DOI:10.17277/jamt. 2024.04.pp.286-295

12. Asai S, Nakamura H, Tanabe M, Sakamoto K. Distribution and dissociation equilibria of phase-transfer catalysts, tetrabutylammonium salts. *Industrial & Engineering Chemistry Research*. 1993;32(7):1438-1441. DOI:10.1021/ie00019a018

13. Zou T, Wang X, Ju H, Zhao L, et al. Controllable molecular packing motif and overlap type in organic nanomaterials for advanced optical properties. *Crystals*. 2018;8(1):22. DOI:10.3390/cryst8010022

14. Mayhall NJ, Raghavachari K, Hratchian HP. ONIOM-based QM:QM electronic embedding method using Löwdin atomic charges: energies and analytic gradients. *The Journal of Chemical Physics*. 2010;132(11):114107. DOI:10.1063/1.3315417

15. Bannwarth C, Ehlert S, Grimme S. GFN2-XTB – an accurate and broadly parametrized self-consistent tight-binding quantum chemical method with multipole electrostatics and density-dependent dispersion contributions. *Journal of Chemical Theory and Computation*. 2019;15(3):1652-1671. DOI:10.1021/acs. jctc.8b01176

16. Grimme S, Hansen A, Ehlert S, Mewes JM. R2SCAN-3C: A “swiss army knife” composite electronic-structure method. *The Journal of Chemical Physics*. 2021;154(6):064103. DOI:10.1063/5.0040021

17. Najibi A, Goerigk L. DFT-D4 counterparts of leading meta-generalized-gradient approximation and hybrid density functionals for energetics and geometries. *Journal of Computational Chemistry*. 2020;41(30):2562-2572. DOI:10.1002/jcc.26411

18. Weigend F, Ahlrichs R. Balanced basis sets of split valence, triple zeta valence and quadruple zeta valence quality for H to Rn: design and assessment of accuracy. *Physical Chemistry Chemical Physics*. 2005;7(18):3297. DOI:10.1039/b508541a

19. Rappoport D, Furche F. Property-optimized gaussian basis sets for molecular response calculations. *The Journal of Chemical Physics*. 2010;133(13):134105. DOI:10.1063/1.3484283

20. Ehlert S, Stahn M, Spicher S, Grimme S. Robust and efficient implicit solvation model for fast semiempirical methods. *Journal of Chemical Theory and Computation*. 2021;17(7):4250-4261. DOI:10.1021/acs. jctc.1c00471

21. Neese F. Software update: the ORCA program system – version 5.0. *WIREs Computational Molecular Science*. 2022;12(5):e1606. DOI:10.1002/wcms.1606

22. Bader RFW. *Atoms in molecules: a quantum theory*. Oxford: Oxford University Press; 1990. 456 p. DOI:10.1093/oso/9780198551683.001.0001

23. Matta CF, Boyd RJ, eds. *The quantum theory of atoms in molecules: from solid state to DNA and drug design*. Wiley; 2007. 568 p. DOI:10.1002/9783527610709

24. Lu T, Chen Q. Interaction region indicator: a simple real space function clearly revealing both chemical bonds and weak interactions. *Chemistry – Methods*. 2021;1(5):231-239. DOI:10.1002/cmtd.202100007

25. Bultinck P, Van Alsenoy C, Ayers PW, Carbó-Dorca R. Critical analysis and extension of the Hirshfeld atoms in molecules. *The Journal of Chemical Physics*. 2007;126(14):144111. DOI:10.1063/1.2715563

26. Breneman CM, Wiberg KB. Determining atom-centered monopoles from molecular electrostatic potentials. The need for high sampling density in formamide conformational analysis. *Journal of Computational Chemistry*. 1990;11(3):361-373. DOI:10.1002/jcc.540110311

27. Lu T, Chen F. Multiwfn: a multifunctional wavefunction analyzer. *Journal of Computational Chemistry*. 2012;33(5):580-592. DOI:10.1002/jcc.22885

28. Becke AD, Edgecombe KE. A simple measure of electron localization in atomic and molecular systems. *The Journal of Chemical Physics*. 1990;92(9):5397–5403. DOI: 10.1063/1.458517

29. Jacobsen H. Localized-orbital locator (LOL) profiles of chemical bonding. *Canadian Journal of Chemistry*. 2008;86(7):695–702. DOI: 10.1139/v08-052

30. Emamian S, Lu T, Kruse H, Emamian H. Exploring nature and predicting strength of hydrogen

bonds: a correlation analysis between atoms-in-molecules descriptors, binding energies, and energy components of symmetry-adapted perturbation theory. *Journal of Computational Chemistry*. 2019;40(32):2868-2881. DOI:10.1002/jcc.26068

31. Parthasarathi R, Subramanian V, Sathyamurthy N. Hydrogen bonding without borders: an atoms-in-molecules perspective. *The Journal of Physical Chemistry A*. 2006;110(10):3349-3351. DOI:10.1021/jp060571z

32. Shahi A, Arunan E. Hydrogen bonding, halogen bonding and lithium bonding: An atoms in molecules and natural bond orbital perspective towards conservation of total bond order, inter- and intra-molecular bonding. *Physical Chemistry Chemical Physics.* 2014;16(42):22935-22952. DOI:10.1039/C4CP02585G

33. Das A, Arunan E. Unified classification of non-covalent bonds formed by main group elements: a bridge to chemical bonding. *Physical Chemistry Chemical Physics*. 2023;25(34):22583-22594. DOI:10.1039/D3CP00370A

34. Pipek J, Mezey PG. A fast intrinsic localization procedure applicable for ab initio and semiempirical linear combination of atomic orbital wave functions. *The Journal of Chemical Physics*. 1989;90(9):4916-4926. DOI:10.1063/1.456588

35. Lehtola S, Jónsson H. Pipek-mezey orbital localization using various partial charge estimates. *Journal of Chemical Theory and Computation*. 2014;10(2):642-649. DOI:10.1021/ct401016x

36. Humphrey W, Dalke A, Schulten K. VMD: visual molecular dynamics. *Journal of Molecular Graphics*. 1996;14(1):33-38. DOI:10.1016/0263-7855(96)00018-5

## Information about the authors / Информация об авторах

**Andrey A. Degtyarev,** Cand. Sc. (Eng.), Associate Professor, Tambov State Technical University (TSTU), Tambov, Russian Federation; ORCID 0000-0003-3690-4565; e-mail: ad.dycost@gmail.com

**Alexandra V. Trishina,** Assistant, TSTU, Tambov, Russian Federation; ORCID 0000-0003-3413-4763; e-mail: koroleva_tambov@mail.ru

**Dariya P. Rostova,** Postgraduate, TSTU, Tambov, Russian Federation; ORCID 0000-0002-2746-3545; e-mail: rostova.dariya@yandex.ru

**Дегтярев Андрей Александрович,** кандидат технических наук, доцент, Тамбовский государственный технический университет (ТГТУ), Тамбов, Российская Федерация; ORCID 0000-0003-3690-4565; e-mail: ad.dycost@gmail.com

**Тришина Александра Викторовна,** ассистент, ТГТУ, Тамбов, Российская Федерация; ORCID 0000-0003-3413-4763; e-mail: koroleva_tambov@mail.ru

**Ростова Дария Павловна,** аспирант, ТГТУ, Тамбов, Российская Федерация; ORCID 0000-0002-2746-3545; e-mail: rostova.dariya@yandex.ru

*Received 27 February 2025; Revised 29 March 2025; Accepted 04 April 2025*

**Copyright:** © Degtyarev AA, Trishina AV, Rostova DP, 2025. This article is an open access article distributed under the terms and conditions of the Creative Commons Attribution (CC BY) license (https://creativecommons.org/licenses/by/4.0/).